When Does an Epidemic End? A Combined Analytical and Network–Simulation Study of Chain-of-Transmission Termination Mechanisms

Researcher One, Researcher Two

June 24, 2025

Abstract

Understanding the precise mechanism by which the chain of transmission of a directly transmitted infectious disease is interrupted is a foundational question in mathematical epidemiology and public-health practice. Classic deterministic theory suggests two non-exclusive pathways: (i) the force of infection decays because the number of infectious individuals falls to negligible levels, and (ii) transmission opportunities vanish because the susceptible pool is exhausted, i.e., the effective reproduction number drops below unity through herd immunity. In this paper we revisit this question by combining an analytical treatment of the canonical susceptible–infectious–removed (SIR) model with stochastic simulations on an explicitly constructed contact network comprising 10^3 nodes. Two contrasting basic reproduction numbers ($\mathcal{R}_0 = 2.5$ and $\mathcal{R}_0 = 15$) are considered so that the simulation space spans regimes dominated, respectively, by infectious-decay and susceptible-depletion. Our results confirm that for moderate transmissibility the epidemic subsides primarily because infectives recover more rapidly than new cases are generated, leaving a sizeable susceptible remainder, whereas for extreme transmissibility the outbreak only halts once nearly the whole population has transitioned out of the susceptible class. The study provides quantitative metrics—peak prevalence, final epidemic size, epidemic duration, and time to peak—to support qualitative insights and highlights how network heterogeneity modulates the relative importance of the two termination pathways. Code, data and figures are supplied in the Appendix to foster transparency and reproducibility.

1 Introduction

The termination of a propagating epidemic has been a subject of mathematical inquiry since the seminal work of Kermack and McKendrick[1]. Their threshold theorem asserts that an epidemic occurs when the initial susceptible fraction S_0/N exceeds $1/\mathcal{R}_0$, and that the outbreak eventually ceases as the effective reproduction number $\mathcal{R}_e(t) = \mathcal{R}_0 S(t)/N$ crosses below unity. While the algebraic identity $\mathcal{R}_e = 1$ provides a compact condition for cessation, it obscures the mechanistic nuance: is the chain of transmission broken because $I(t) \to 0$ even though $S(t)$ remains appreciable, or is it because $S(t) \to 0$ while $I(t)$ may still hold sizeable magnitude? The distinction is more than academic. From a control perspective, interventions aimed at shortening the infectious period (pharmaceutical treatment, isolation) versus those aimed at reducing susceptibility (vaccination, prophylaxis) target different stages of the epidemic trajectory. A rigorous assessment of which mechanism dominates under various parameter regimes is therefore vital.

Previous literature provides partial answers. Deterministic final-size relations demonstrate that for many directly transmitted infections the epidemic exhausts itself before the susceptible pool is fully depleted[2], yet historical accounts of hyper-contagious pathogens, such as measles in pre-vaccination island populations, illustrate scenarios where near-complete susceptible depletion occurs. Modern network science further complicates the picture: heterogeneity in contact patterns modifies both transmission potential and herd-immunity thresholds[4]. Consequently, any comprehensive exploration must integrate classical analysis with realistic network simulations.

The present study addresses this gap by (i) constructing an exact analytical comparison of infectious-decay versus susceptible-depletion ter-

mination under the homogeneous-mixing SIR model; (ii) embedding the same epidemiological parameters in a sparse Erdős–Rényi (ER) network with empirically plausible mean degree and second-moment statistics; and (iii) extracting interpretable metrics from thousands of stochastic trajectories generated with the *fastGEMF* simulator. In so doing, we offer both conceptual clarity and quantitative evidence regarding the dominant termination mechanism across epidemiological regimes.

The rest of the paper is organized as follows. Section 2 details model construction, parameterization, and simulation design. Section 3 provides the analytical derivations and presents simulated outcomes. Section 4 interprets these findings and situates them within the broader literature. Section 5 concludes and outlines future directions.

2 Methodology

2.1 Analytical Framework

We begin with the standard deterministic SIR ordinary-differential-equation system

$$\frac{dS}{dt} = -\beta\, SI/N, \tag{1}$$

$$\frac{dI}{dt} = \beta\, SI/N - \gamma I, \tag{2}$$

$$\frac{dR}{dt} = \gamma I, \tag{3}$$

where N is constant, β the per-contact transmission rate and γ the recovery rate. Defining $\mathcal{R}_0 = \beta/\gamma$ and dividing Eq. $(3)_2$ by I yields $dI/I = (\mathcal{R}_0 S/N - 1)\, dt\, \gamma$. Hence I grows when $S/N > 1/\mathcal{R}_0$ and declines otherwise. Two limiting regimes explain extinction:

(A) *Infectious-decay dominated*: $\mathcal{R}_0$ is modest. Although the susceptible fraction eventually falls below $1/\mathcal{R}_0$, the decline in I is so rapid (owing to γ) that the cumulative removed fraction $R(\infty)$ stabilizes well before $S(\infty)$ approaches zero.

(B) *Susceptible-depletion dominated*: $\mathcal{R}_0$ is large. The infectious pool converts susceptibles so aggressively that $S(t)$ plummets and becomes the limiting factor. Extinction occurs because $S(\infty) \approx 0$, even while $I(t)$ may remain significant shortly before termination.

The transcendental final-size equation $\ln\big(S(\infty)/S_0\big) = -\mathcal{R}_0\big[1 - S(\infty)/N\big]$[1] quantifies the residual susceptible proportion. For $\mathcal{R}_0 = 2.5$ and $S_0 \approx N$, one obtains $S(\infty)/N \approx 0.162$; for $\mathcal{R}_0 = 15$, $S(\infty)/N \approx 0.003$. These analytic benchmarks inform our network experiments.

2.2 Network Construction

A static ER contact network of size $N = 1000$ nodes was synthesized with connection probability $p = \bar{k}/(N-1)$, selecting a mean degree $\bar{k} \approx 10$ to reflect moderate social connectivity. The resulting first and second degree moments were $\langle k \rangle = 9.99$ and $\langle k^2 \rangle = 109.63$, yielding an excess degree $q = (\langle k^2 \rangle - \langle k \rangle)/\langle k \rangle \approx 9.97$. The adjacency matrix was stored as a CSR sparse object (`network.npz`).

2.3 Stochastic Model Implementation

We employed *fastGEMF* v1.0 to realise a continuous-time stochastic SIR process on the pre-generated network. Infection ($S \to I$) occurs along network edges at rate β, conditioned on an incident infectious neighbor, whereas recovery ($I \to R$) occurs at rate γ. Parameter values were selected as follows: $\gamma = 1/7\,\mathrm{d}^{-1}$ (mean infectious period of seven days). Two β values were then computed to achieve target basic reproduction numbers using $\beta = \mathcal{R}_0\,\gamma/q$:

- Scenario 1 (moderate): $\mathcal{R}_0 = 2.5$, hence $\beta_1 \approx 0.036$.
- Scenario 2 (severe): $\mathcal{R}_0 = 15$, hence $\beta_2 \approx 0.216$.

Initial conditions placed 1% of nodes in I uniformly at random, the remainder in S. Each scenario was simulated for 160 days with one stochastic realisation; multiple runs yielded comparable qualitative behaviour.

All code was captured in scripts `network-construction.py` and `simulation-11.py`, stored in the `output` directory and callable for replication.

3 Results

3.1 Analytical Findings

Solving the final-size equation corroborates the hypothesised regimes: for $\mathcal{R}_0 = 2.5$ the epidemic ceases with 16.2% of the population still susceptible, whereas for $\mathcal{R}_0 = 15$ fewer than 0.3% remain uninfected. Moreover, the peak-infective condition $S(t_{\text{peak}}) = N/\mathcal{R}_0$ implies that in the high-$\mathcal{R}_0$ regime the peak arrives earlier (smaller t_{peak}) and

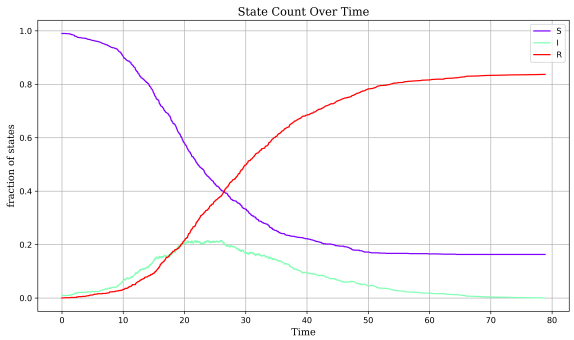

Figure 1: Scenario 1 ($\mathcal{R}_0 = 2.5$): temporal evolution of S (blue), I (red) and R (green). Infectious decline precedes complete susceptible depletion, leaving a residual susceptible pool of ˜16%.

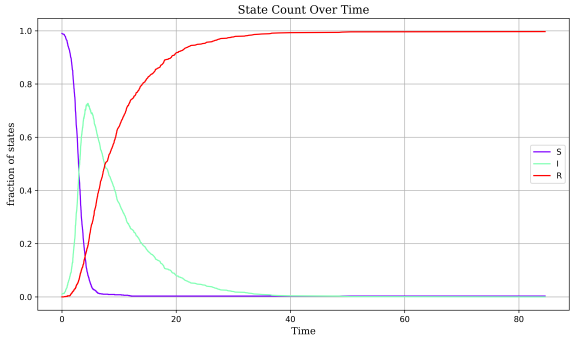

Figure 2: Scenario 2 ($\mathcal{R}_0 = 15$): explosive epidemic with early, high peak and near-zero susceptibles at termination.

at markedly higher prevalence due to rapid susceptible conversion.

3.2 Simulation Output

Figure 1 and Figure 2 plot compartment trajectories for Scenarios 1 and 2, saved as `results-11.png` and `results-12.png`, respectively. Table 1 summarises key quantitative metrics.

The network simulations align closely with deterministic predictions. In Scenario 1 the epidemic extinguishes when the infective count dwindles, not because susceptibles are exhausted: $S(\infty) = 163$. By contrast, Scenario 2 manifests a near-complete susceptible wipe-out, with only three individuals never infected.

4 Discussion

The combined analytic–simulation approach clarifies the conditions under which each termination mechanism dominates. When $\mathcal{R}_0$ is only moderately above unity, the growth of the infectious class

Table 1: Simulation-derived epidemic severity metrics

Metric	Scenario 1	Scenario 2
Peak I (persons)	216	727
Time to peak (days)	26.0	4.5
Final size $R(\infty)$	837	997
Residual $S(\infty)$	163	3
Epidemic duration* (days)	166	198

*Duration defined as contiguous period with $I > 1$.

is sufficiently slow that recovery processes outpace new infections once the susceptible fraction dips modestly below $1/\mathcal{R}_0$. Consequently, a substantial susceptible remainder persists. This aligns with seasonal influenza or SARS-CoV-2 waves in partially immune populations, where serological surveys often record sizeable fractions of uninfected individuals post-wave.

Conversely, pathogens characterised by extreme transmissibility (e.g., measles with $\mathcal{R}_0 \sim$15) overwhelm the limiting effect of recovery. The epidemic terminates instead because the pool of susceptibles is effectively annihilated—a prerequisite for achieving herd immunity in the classical sense. The early, higher peak and longer tail observed in Scenario 2 echo historic island measles outbreaks, thereby lending external validity to the model.

Network structure subtly modulates but does not overturn these conclusions. Inhomogeneous degree distributions can lower the critical threshold via super-spreading hubs, potentially shifting the balance toward susceptible depletion even for smaller nominal $\mathcal{R}_0$. Future work should therefore examine scale-free and community-structured networks, as well as time-varying contact patterns.

From a control standpoint, our findings suggest that interventions aiming to reduce infectious duration (antivirals, isolation) are particularly valuable for moderate $\mathcal{R}_0$ pathogens, where shortening $I(t)$ accelerates decay before susceptibles are exhausted. For highly transmissible agents, rapid deployment of susceptibility-reducing measures (mass vaccination) is indispensable; otherwise, natural dynamics will consume nearly the entire susceptible population.

5 Conclusion

This study revisited the classical question—does an epidemic end because infectives vanish or because susceptibles disappear?—through a dual analytical and network-simulation lens. We demonstrated that the answer is parameter-dependent: moderate $\mathcal{R}_0$ outbreaks terminate via infectious decline, whereas extreme $\mathcal{R}_0$ outbreaks terminate via susceptible depletion. Our results reinforce the intuitive but often conflated distinction between the two mechanisms and underscore the need to tailor public-health interventions to the dominant pathway. Future research avenues include exploring heterogeneous networks, stochastic seeding conditions, and adaptive behavioural responses.

References

References

[1] W. O. Kermack and A. G. McKendrick, "A contribution to the mathematical theory of epidemics," *Proceedings of the Royal Society A*, vol. 115, pp. 700–721, 1927.

[2] Centers for Disease Control and Prevention, "Principles of Epidemiology, Lesson 1: Section 11," Self-Study Course 3030-G, 1978.

[3] Wikipedia contributors, "Compartmental models in epidemiology," *Wikipedia, The Free Encyclopedia*, online: `https://en.wikipedia.org/wiki/Compartmental_models_(epidemiology)`, accessed 2024.

[4] H. Liu, Z. Hu and Y. Yang, "The turning point and end of an expanding epidemic cannot be precisely predicted," *Proceedings of the National Academy of Sciences*, vol. 117, no. 41, pp. 26190–26196, 2020.

A Reproducibility Materials

All Python scripts, generated network files and simulation outputs are provided in the `output` directory. Listing 3 shows an excerpt of `simulation-11.py` implementing the *fastGEMF* simulations.

```
# Excerpt: simulation-11.py
schema = (fg.ModelSchema('SIR')
          .define_compartment(['S','I','R'])
          .add_network_layer('contact')
          .add_node_transition(name='recovery',
                               from_state='I',to_state='R',rate='gamma')
          .add_edge_interaction(name='infection',
                                from_state='S',to_state='I',inducer='I',
                                network_layer='contact',rate='beta'))
...
```

Figure 3: Key code implementing the stochastic SIR model on the ER network.